Electronic Supplementary Material (ESI) for Nanoscale.

Supporting Information

A two-dimensional hybrid with molybdenum disulfide nanocrystals strongly coupled on nitrogen-enriched graphene via mild temperature pyrolysis for high performance lithium storage

Yanping Tang,† Dongqing Wu,† Yiyong Mai,† Hao Pan,† Jing Cao,† Chongqing Yang,† Fan Zhang,† Xinliang Feng†‡**

†School of Chemistry and Chemical Engineering, Shanghai JiaoTong University, 200240, Shanghai, P. R. China, †‡Fachrichtung Chemie und Lebensmittelchemie, Technische Universitaet Dresden, 01062 Dresden, Germany.

* wudongqing@sjtu.edu.cn, xinliang.feng@tu-dresden.de.

Experimental Section

Materials and synthesis: Flake graphite was purchased from Aldrich. All other chemicals were purchased from Aladdin Reagent (Shanghai) and used without further purification.

Preparation of graphene oxide (GO): GO was synthesized from natural graphite flakes based on a modified Hummers method.[3] A homogeneous GO aqueous dispersion (2.5 mg mL^{-1}) was then ready for use.

Preparation of protonated g-C_3N_4 (g-C_3N_4-H^+): g-C_3N_4 was first obtained by thermal annealing of urea at 550 ℃ for 2h under air with a heating rate of 2 ℃/min. Protonated g-C_3N_4 was prepared via sonication of g-C_3N_4 with HCl (37%) for 3 h at room temperature.

Synthesis of MoS_2/$NG_{g\text{-}C_3N_4}$: GO aqueous dispersion (20 mL, 50mg) was first diluted in de-ionized (DI) water (200 mL) with addition of g-C_3N_4-H^+ (100 mg) and sonicated for 1 h to obtain a flocculation of GO and g-C_3N_4-H^+ (g-C_3N_4-H^+/GO), which was then fed with $Na_2MoO_4 \cdot 2H_2O$ (300 mg) and stirred at 90 ℃ for 12 h. The following addition of $Na_2S \cdot 9H_2O$ (1.5g) and HCl (4 mL) immediately led to the formation of brownish precipitate (MoS_3/g-C_3N_4-H^+/GO), which was collected by filtration, freeze-dried, and finally treated at 550 ℃ for 3h under N_2 with a heating rate of 5 ℃/min to obtain MoS_2/$NG_{g\text{-}C_3N_4}$. Moreover, another sample as MoS_2/$NG_{g\text{-}C_3N_4}$ (10:100:50) could be obtained when 10 mg $Na_2MoO_4 \cdot 2H_2O$ was added with $Na_2MoO_4 \cdot 2H_2O$:g-C_3N_4-H^+:GO (10:100:50). As the optimized ratio, $Na_2MoO_4 \cdot 2H_2O$:g-C_3N_4-H^+:GO (300:100:50) was adopted to achieve appropriate MoS_2 loading and high content nitrogen doping in graphene.

Synthesis of MoS_2/G: GO aqueous dispersion (20 mL, 50mg) was first diluted in DI water (200 mL) with subsequent addition of $Na_2MoO_4 \cdot 2H_2O$ (300 mg). The mixture was then stirred at 90 ℃ for 12 h. The following addition of $Na_2S \cdot 9H_2O$ (1.5g) and HCl (4 mL) immediately led to the formation of brownish precipitate (MoS_3/GO), which was collected by filtration, freeze-dried, and finally treated at 550 ℃ for 3h under N_2 with a heating rate of 5 ℃/min to obtain MoS_2/G.

Synthesis of MoS_2/NGurea: MoS_3/GO obtained in above process was re-dispersed in DI water (50 mL) with an addition of urea (1 g) (10 times the mass of g-C_3N_4 in MoS_3/g-C_3N_4-H^+/GO). Water was then evaporated via stirring the mixture at 80℃. The resulting solid mixture was treated at 550 ℃ for 3h under N_2 with a heating rate of 5 ℃/min to obtain MoS_2/NGurea.

Synthesis of MoS_2: Solution with $Na_2MoO_4 \cdot 2H_2O$ (300 mg) dispersed in DI water (200 mL) was stirred at 90 ℃. $Na_2S \cdot 9H_2O$ (1.5g) and HCl (4 mL) were then added with brownish precipitate formed (MoS_3), which was collected by filtration, freeze-dried, and finally treated at 550 ℃ for 3h under N_2 with a heating rate of 5 ℃/min to obtain MoS_2.

Characterizations: Zeta potential was acquired on ZS90 (Malvern Instruments Ltd, UK). XRD measurement was carried out on a D/max-2500 X-ray diffractometer (Rigaku Corporation, Japan) using Cu K_α radiation (λ=0.1542 nm). FTIR spectra were recorded using Spectrum 100 spectrometer (Perkin Elmer, Inc., USA). SEM images, EDX and elemental mapping were acquired using NOVA NanoSEM 230 microscope (FEI, USA). TEM images and SAED pattern were conducted on JEM-2100 microscope (JEOL Ltd., Japan). AFM images were taken on NanoNavi probe station in tapping mode (DI, USA).

Nitrogen physisorption measurement was carried on Autosorb-iQA3200-4 sorption analyzer (Quantatech Co., USA). TGA curves were monitored on a Q5000IR apparatus (TA Instruments, USA). XPS experiment was carried out on AXIS Ultra DLD system from Kratos with Al Kα radiation as X-ray source for radiation. Raman measurement was conducted on an Invia/Reflrx Laser Micro-Raman spectrometer (Renishaw, England) excited by a laser beam of 532 nm.

Electrochemical Measurements:

Electrochemical tests of LIBs were performed under ambient temperature using two-electrode 2032 coin-type cell. Pure lithium foil was used as the counter electrode. A microporous polypropylene membrane was used as the separator. The electrolyte consisting of a solution of 1 M $LiPF_6$ in ethylene carbonate (EC)/dimethyl carbonate (DMC) (1:1 by volume) was obtained from Ube Industries Ltd. The working electrodes were prepared by mixing the MoS_2 based materials (MoS_2/NG$_{g\text{-}C_3N_4}$, MoS_2/NG$_{urea}$, or MoS_2/G), carbon black (Super-P), and poly(vinyl difluoride) (PVDF) at a weight ratio of 8:1:1 and pasting the mixture on pure copper foil (99.6%). The electrode was dried at 60 °C for 12 h in a vacuum oven. The electrode was cut into Φ11 mm sheets and pressed. The amount of active materials loaded on the electrode was ~1.5 mg·cm^{-2}. The cells were assembled in an argon-filled glove box with the concentrations of moisture and oxygen below 1 ppm. CV tests were conducted on a CHI760 electrochemistry workstation at a scan rate of 0.1 mV/s. AC impedance spectroscopy was obtained by applying a sine wave with amplitude of 1.5 V over the frequency range from 100 kHz to 0.01 Hz. Galvanostatic charge/discharge measurements were conducted on a battery tester (Land CA2001A) at various current rates in a potential range of 0.01-3.0 V vs. Li/Li$^+$. The capacity was calculated based on the total mass of the materials.

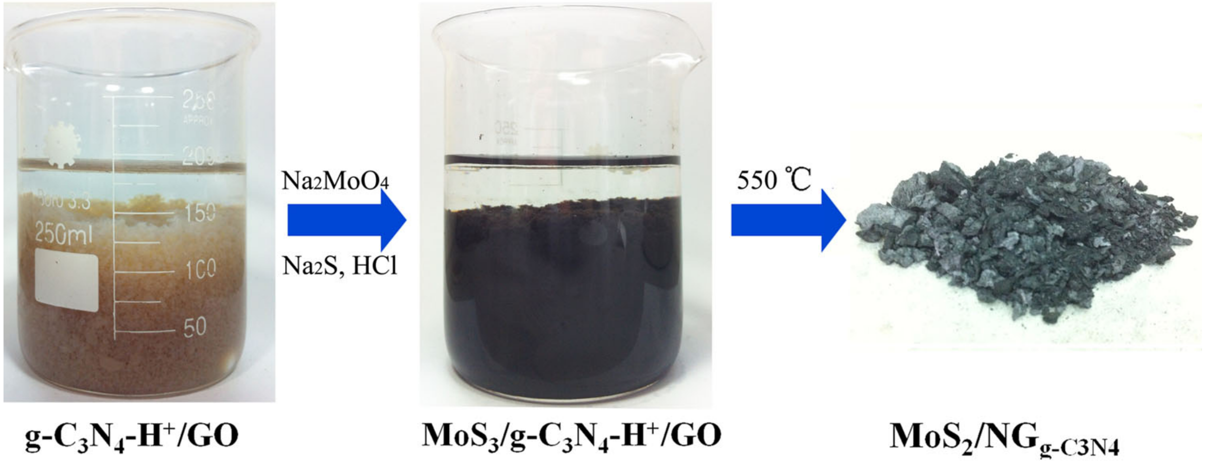

Fig. S1 Photo images of g-C_3N_4-H^+/GO flocculation, MoS_3/g-C_3N_4-H^+/GO precipitate and the product of $MoS_2/NG_{g\text{-}C_3N_4}$.

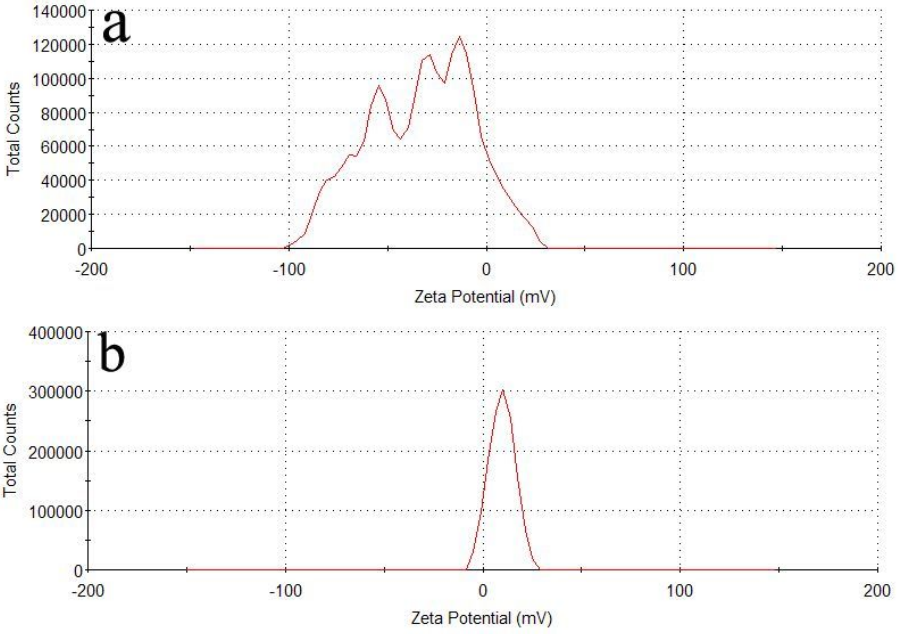

Fig. S2 Zeta Potentials of (a) 0.25 mg/L GO aqueous solution, (b) 0.5 mg/L g-C_3N_4-H^+ aqueous solution.

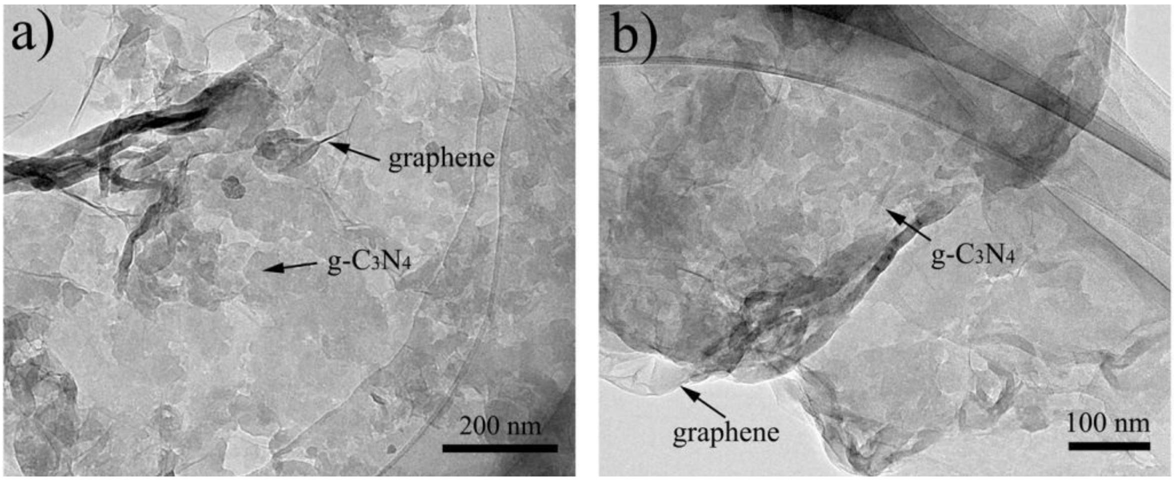

Fig. S3 TEM images of $g\text{-}C_3N_4\text{-}H^+/GO$.

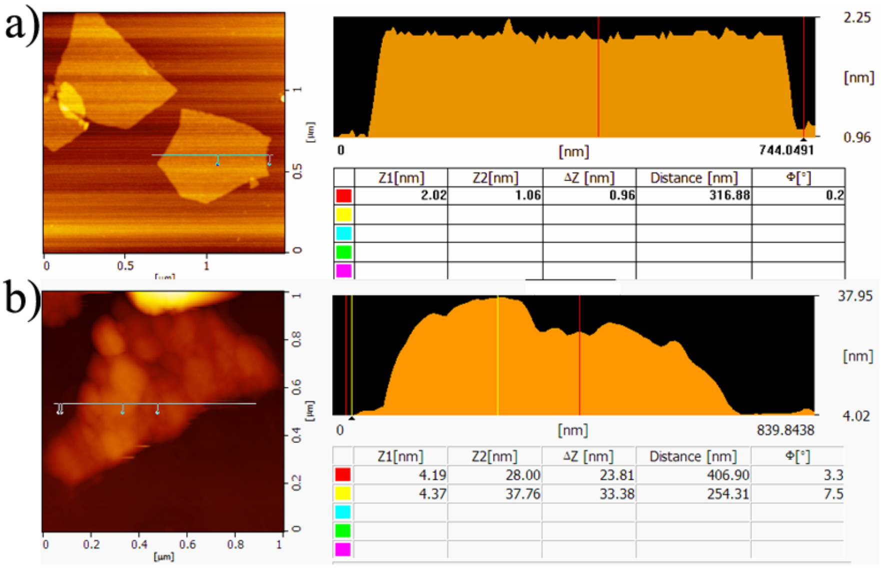

	Z1[nm]	Z2[nm]	ΔZ [nm]	Distance [nm]	Φ[°]
🟥	2.02	1.06	0.96	316.88	0.2
🟨					
🟦					
🟩					
🟪					

	Z1[nm]	Z2[nm]	ΔZ [nm]	Distance [nm]	Φ[°]
🟥	4.19	28.00	23.81	406.90	3.3
🟨	4.37	37.76	33.38	254.31	7.5
🟦					
🟩					
🟪					

Fig. S4 AFM images and corresponding height profiles of a) GO, and b) $g\text{-}C_3N_4\text{-}H^+/GO$.

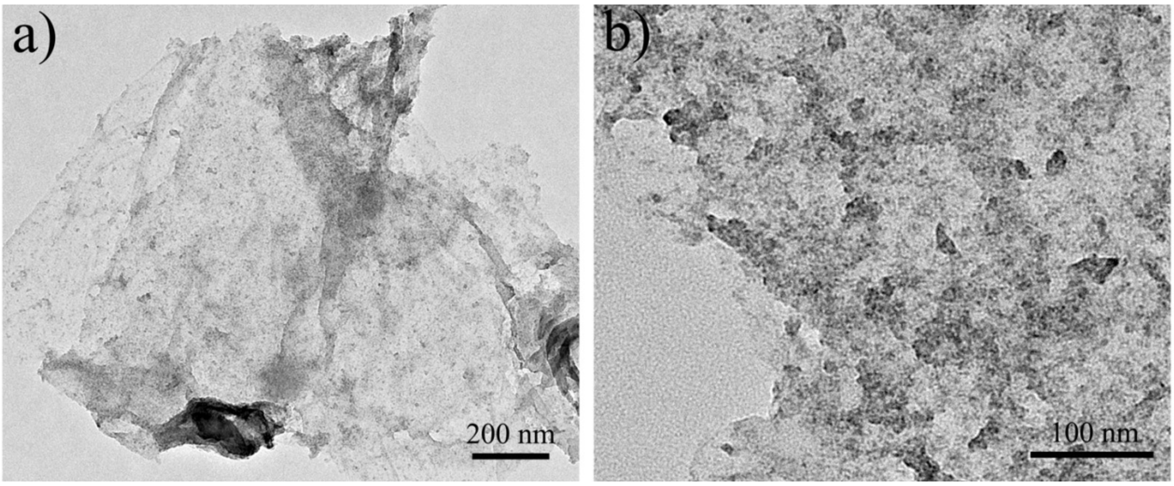

Fig. S5 TEM images of $MoS_3/g\text{-}C_3N_4\text{-}H^+/GO$. MoO_4^{2-} ions can be integrated on the surface of $g\text{-}C_3N_4\text{-}H^+$ via ionic interactions to form MoS_3 nanoparticles by its precipitation with S^{2-} in acid environment.

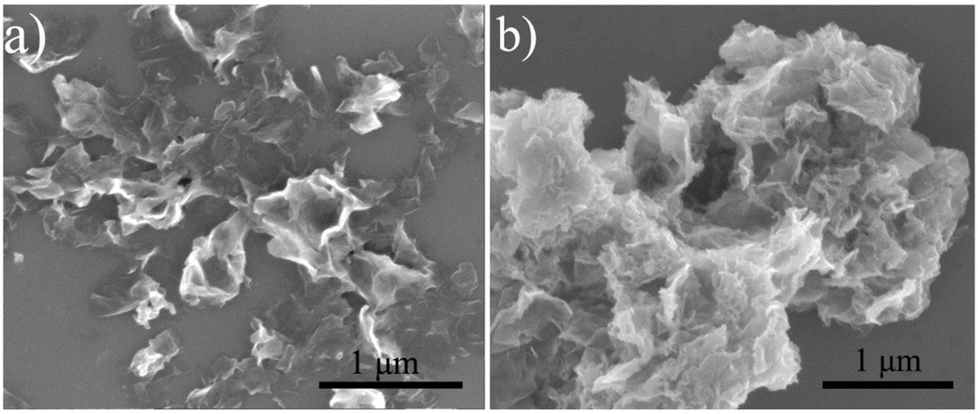

Fig. S6 SEM images of $MoS_2/NG_{g\text{-}C_3N_4}$.

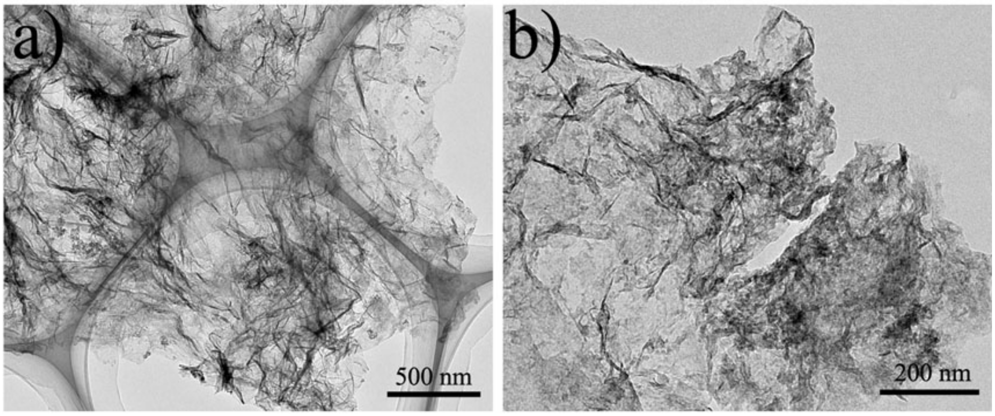

Fig. S7 TEM images of $MoS_2/NG_{g\text{-}C_3N_4}$.

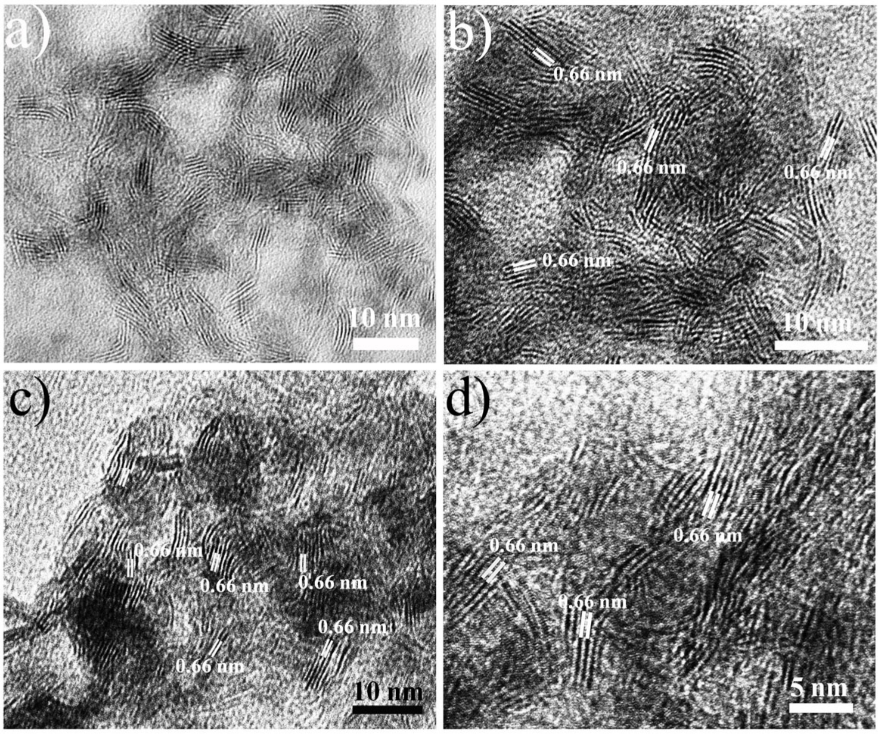

Fig. S8 HRTEM images of $MoS_2/NG_{g\text{-}C_3N_4}$ with uniform (002) d-spacing of 0.66 nm.

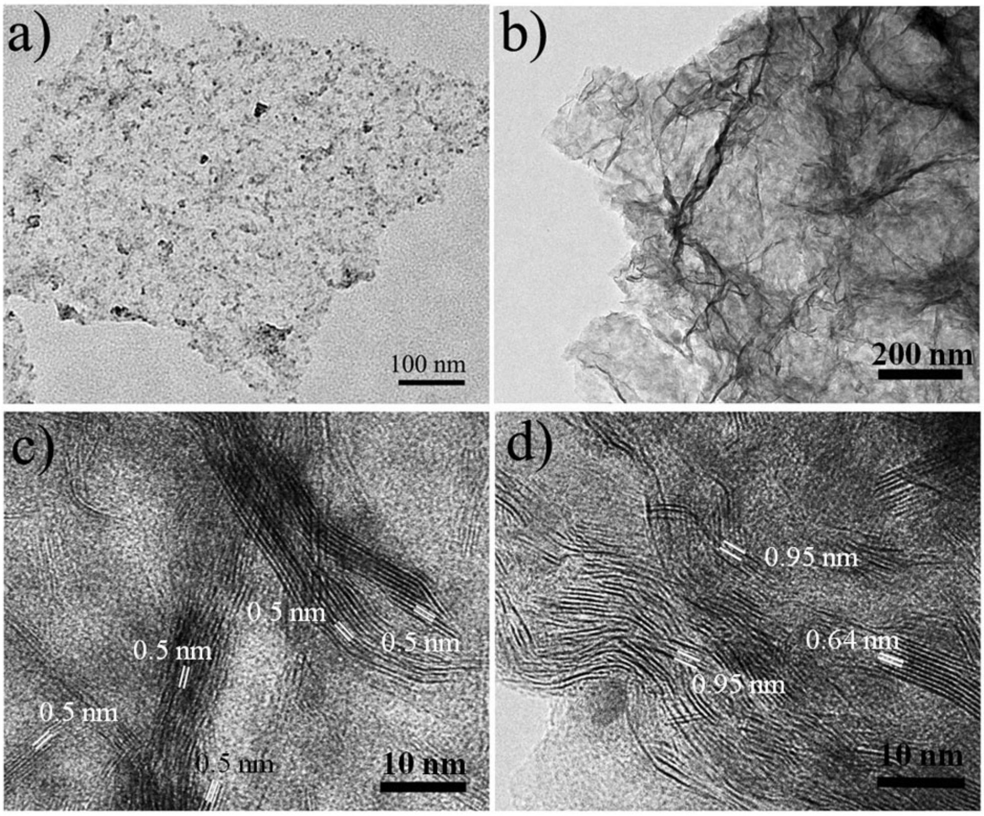

Fig. S9 (a) TEM image of MoS_3/GO, MoO_4^{2-} ions can also be incorporated on GO, but via interactions between oxygen-containing groups on GO and the high valence Mo center;[1] (b) TEM, (c), and (d) HRTEM images of MoS_2/G with irregular (002) d-spacings.

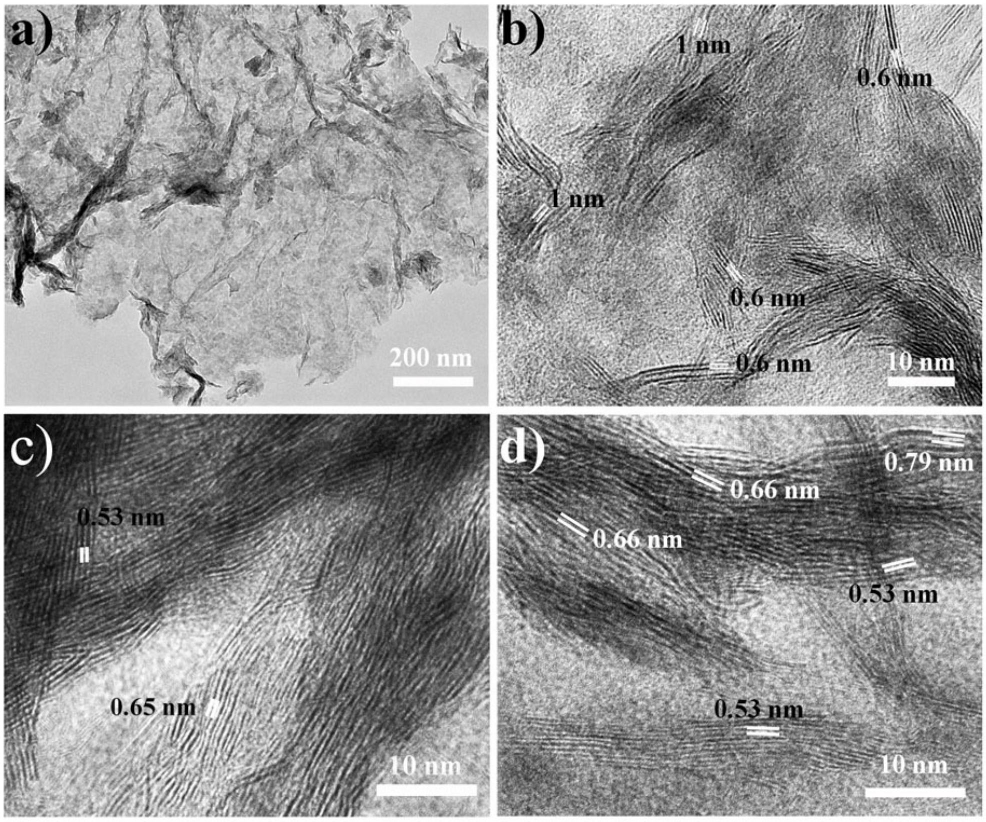

Fig. S10 (a) TEM, (b-d) HRTEM images of MoS_2/NGurea with irregular (002) d-spacings.

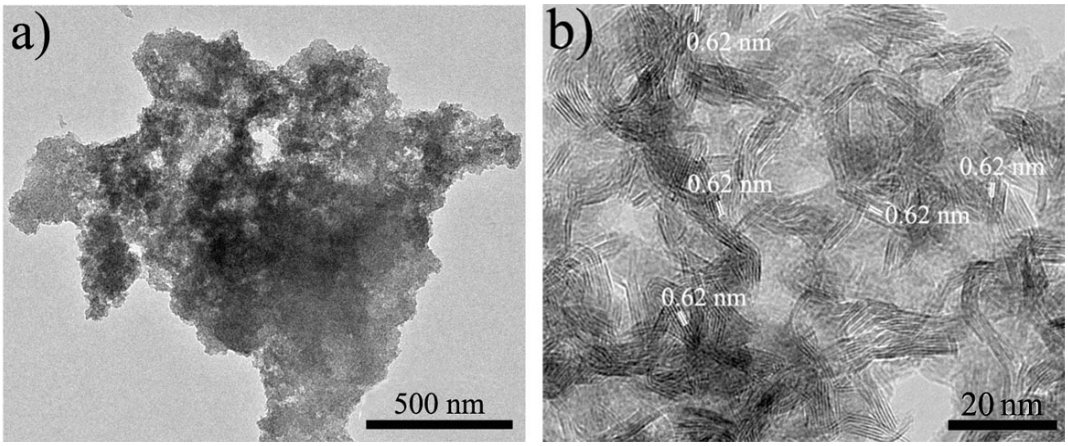

Fig. S11 TEM images of (a) MoS_3; (b) bare MoS_2 with (002) d-spacing of 0.62 nm.

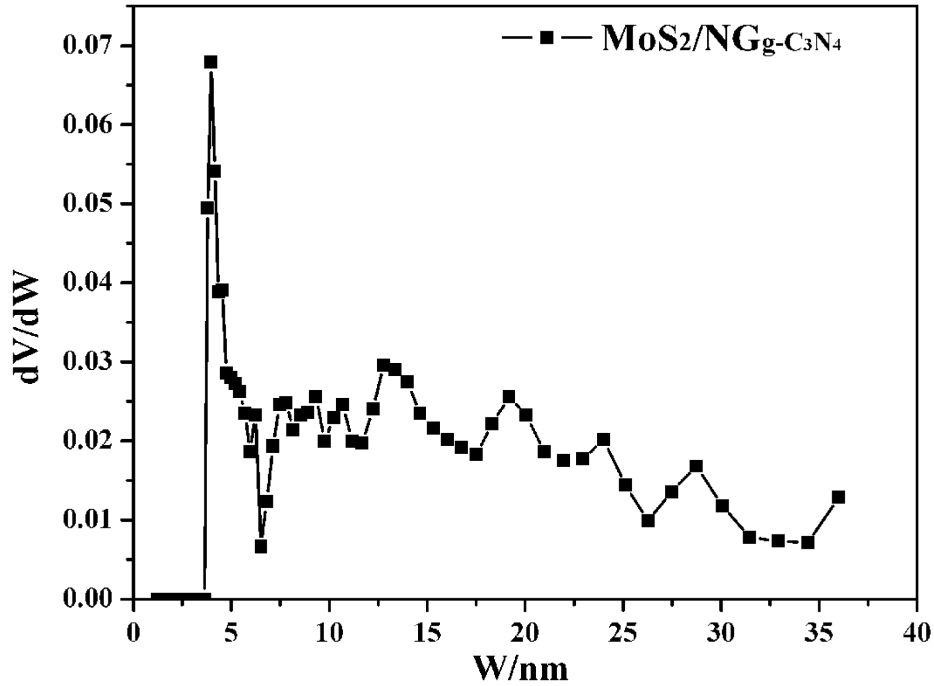

Fig. S12 Pore size distribution of $MoS_2/NG_{g\text{-}C_3N_4}$ according to DFT method. The pores are in the mesoporous range.

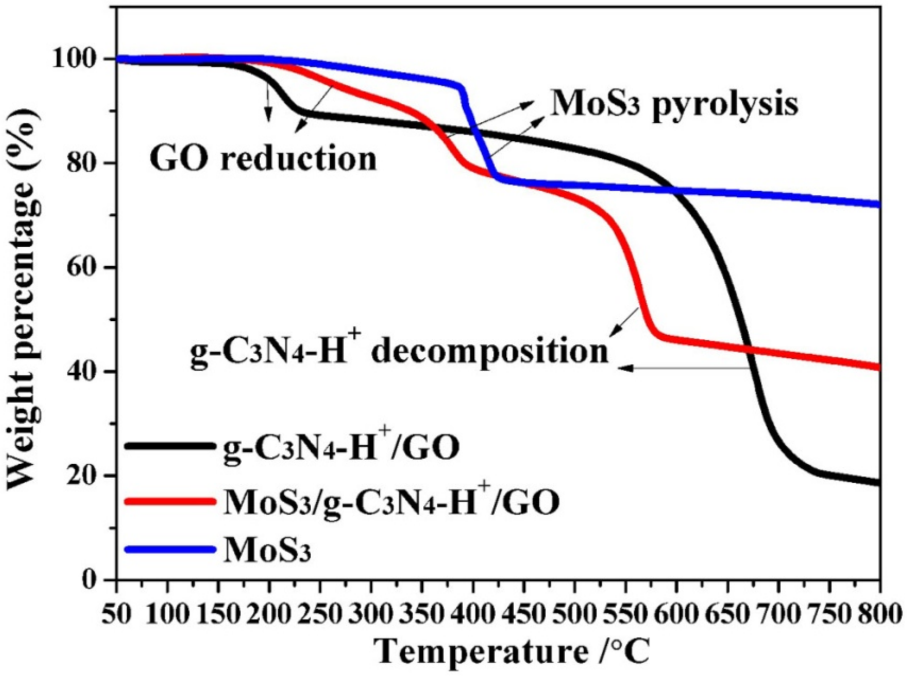

Fig. S13 TGA curves of MoS_3, g-C_3N_4-H^+/GO, MoS_3/g-C_3N_4-H^+/GO under N_2 at a heating rate of 5 °C/min.

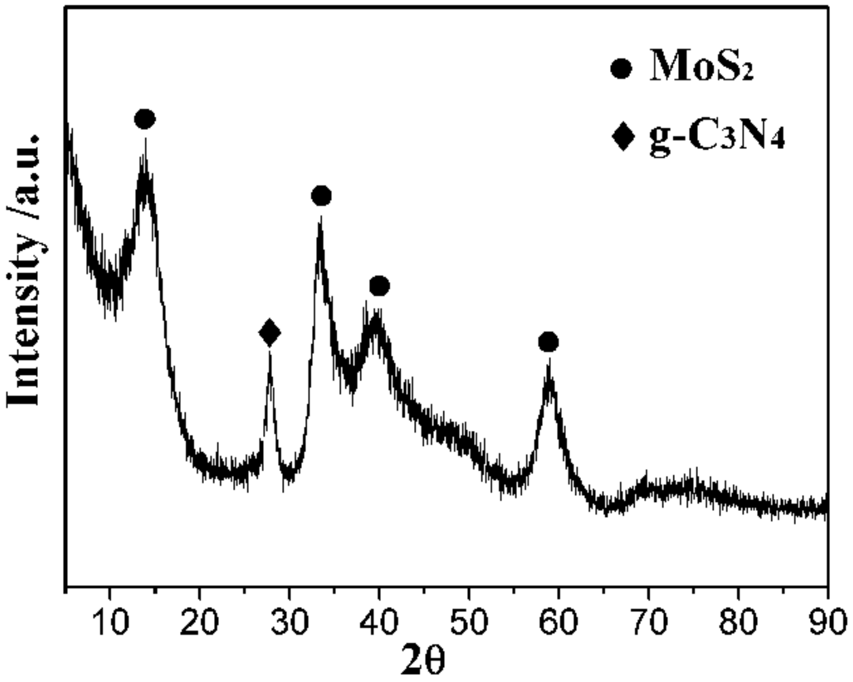

Fig. S14 XRD pattern of the resulting material after thermal treatment of MoS_3/g-C_3N_4-H^+/GO at 400 °C for 3 hours under N_2.

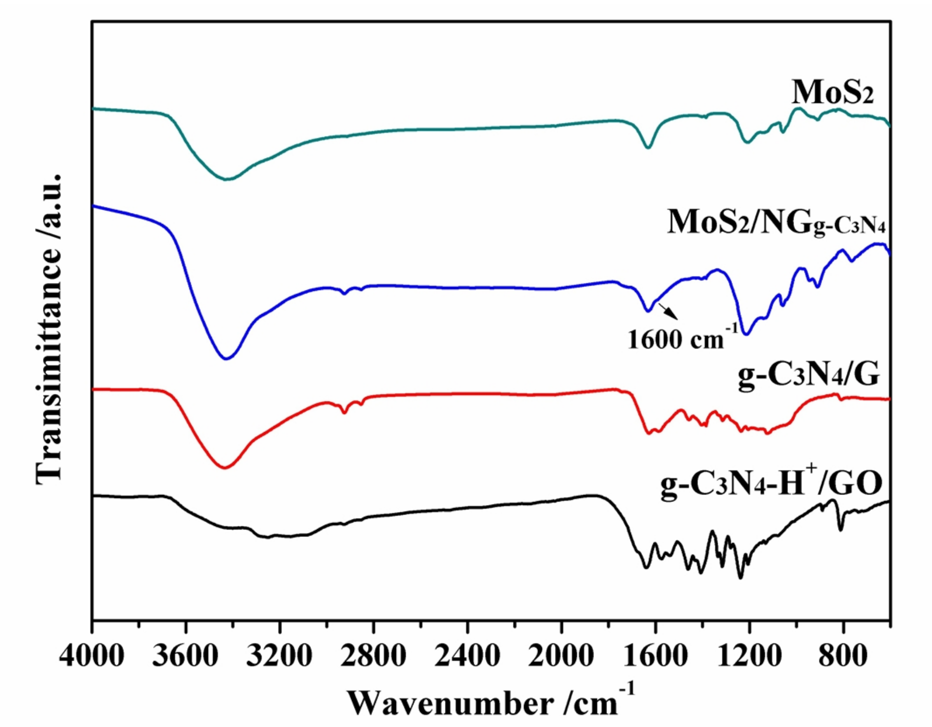

Fig. S15 FTIR spectra of g-C_3N_4-H^+/GO, g-C_3N_4/G, MoS_2/NGg-C_3N_4 and pure MoS_2. g-C_3N_4-H^+/GO displays typical CN heterocycle stretches in 1200-1680 cm^{-1} and s-triazine vibration at 800 cm^{-1} for g-C_3N_4. These features are maintained for g-C_3N_4/G, which is obtained by treatment of g-C_3N_4-H^+/GO at 550 °C for 3h in N_2.[2] In contrast, after treatment of MoS_3/g-C_3N_4-H^+/GO at 550 °C, the g-C_3N_4 features are absent for MoS_2/NGg-C_3N_4 with other arised peaks for MoS_2 and 1600 cm^{-1} peak for C=N in graphene,[3] confirming the complete decomposition of g-C_3N_4-H^+.

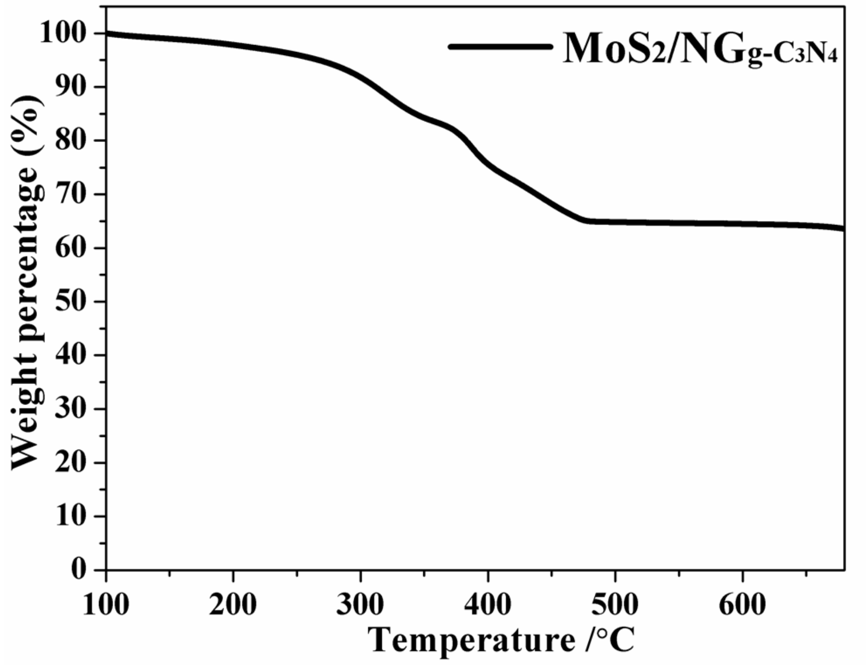

Fig. S16 TGA of MoS_2/NGg-C_3N_4 under air at a heating rate of 5 °C /min.

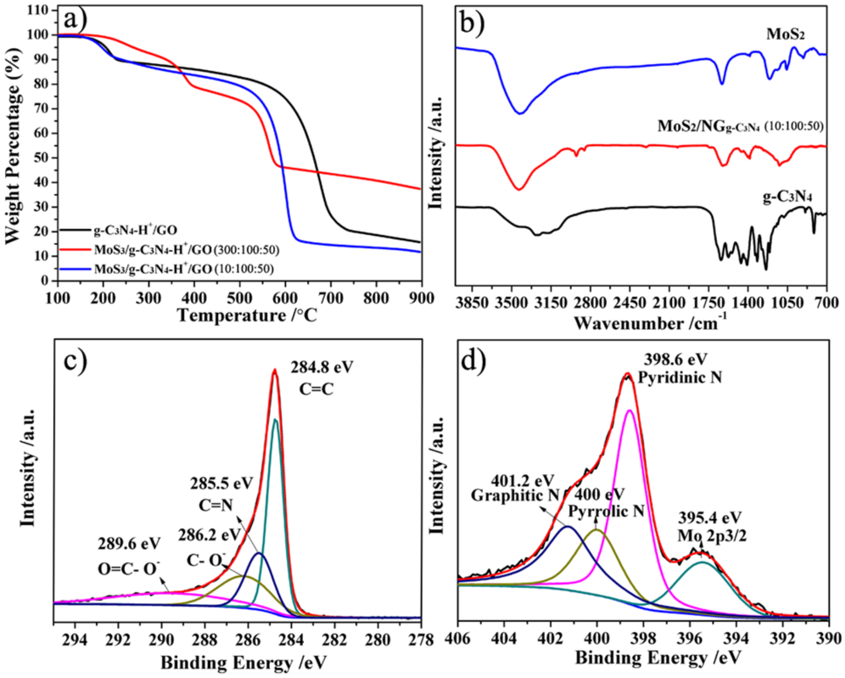

Fig. S17 a) TGA curves of g-C_3N_4-H^+/GO, MoS_3/g-C_3N_4-H^+/GO (10:100:50), MoS_3/g-C_3N_4-H^+/GO (300:100:50) under N_2 at a heating rate of 5 °C/min; b) FTIR spectra of g-C_3N_4, MoS_2/NG$_{g\text{-}C_3N_4}$(10:100:50) and pure MoS_2; Core-level XPS spectra of c) C 1s; d) N 1s and Mo 2p for MoS_2/NG$_{g\text{-}C_3N_4}$(10:100:50). TGA of MoS_3/g-C_3N_4-H^+/GO (10:100:50) also shows promoted decomposition of g-C_3N_4-H^+ at 500-600 °C. FTIR functionalities of g-C_3N_4 are also in absence for MoS_2/NG$_{g\text{-}C_3N_4}$(10:100:50). These results show that complete g-C_3N_4-H^+ decomposition can also be promoted by a small amount of MoS_3 in the precursor and successfully doped nitrogen into graphene.

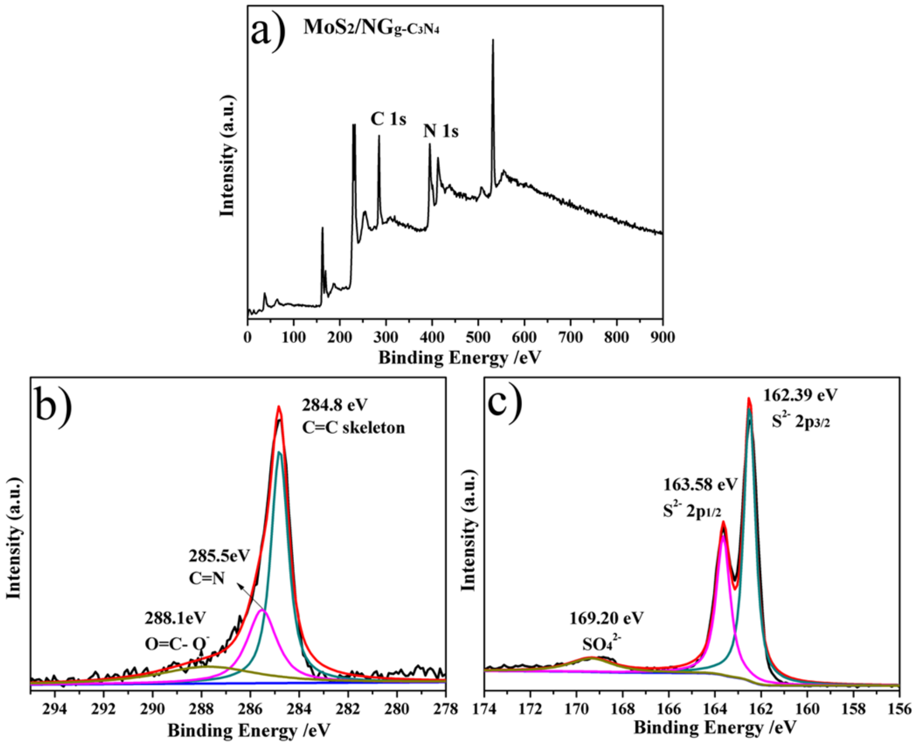

Fig. S18 XPS (a) survey spectra; core-level spectra of (b) C 1s; (c) S 2p for MoS_2/NG$_{g\text{-}C_3N_4}$.

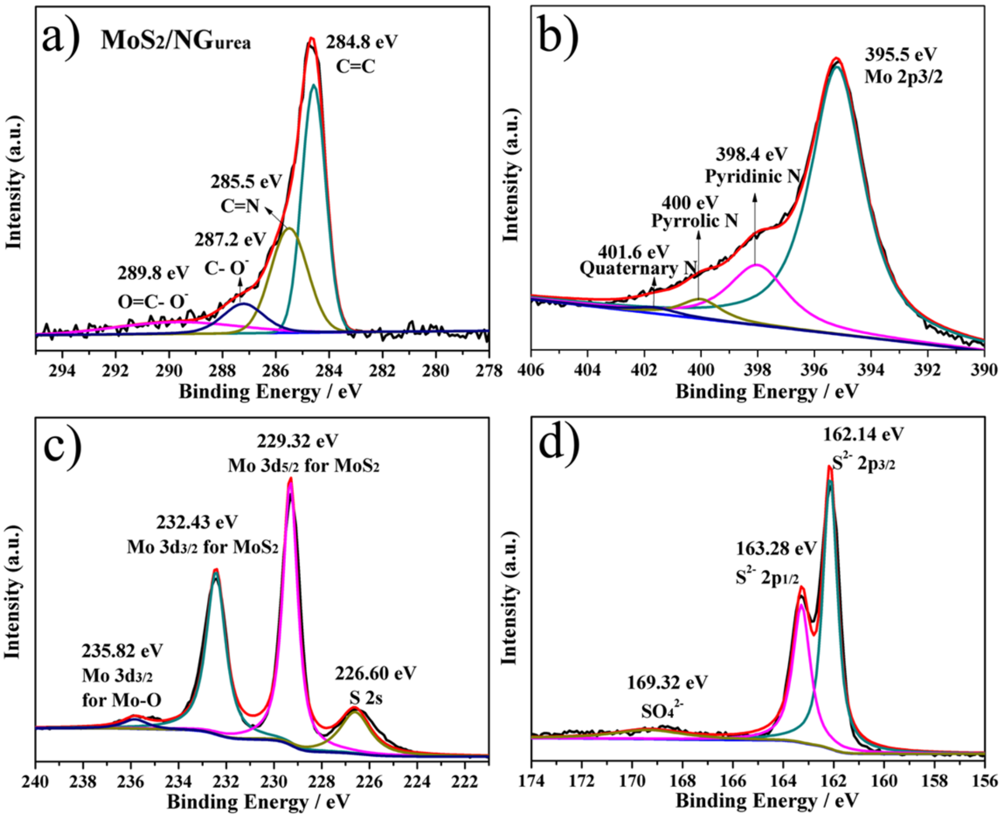

Fig. S19 Core-level XPS spectra of (a) C 1s; (b) N 1s and Mo 2p; (c) Mo 3d and S 2s; (d) S 2p for MoS_2/NGurea.

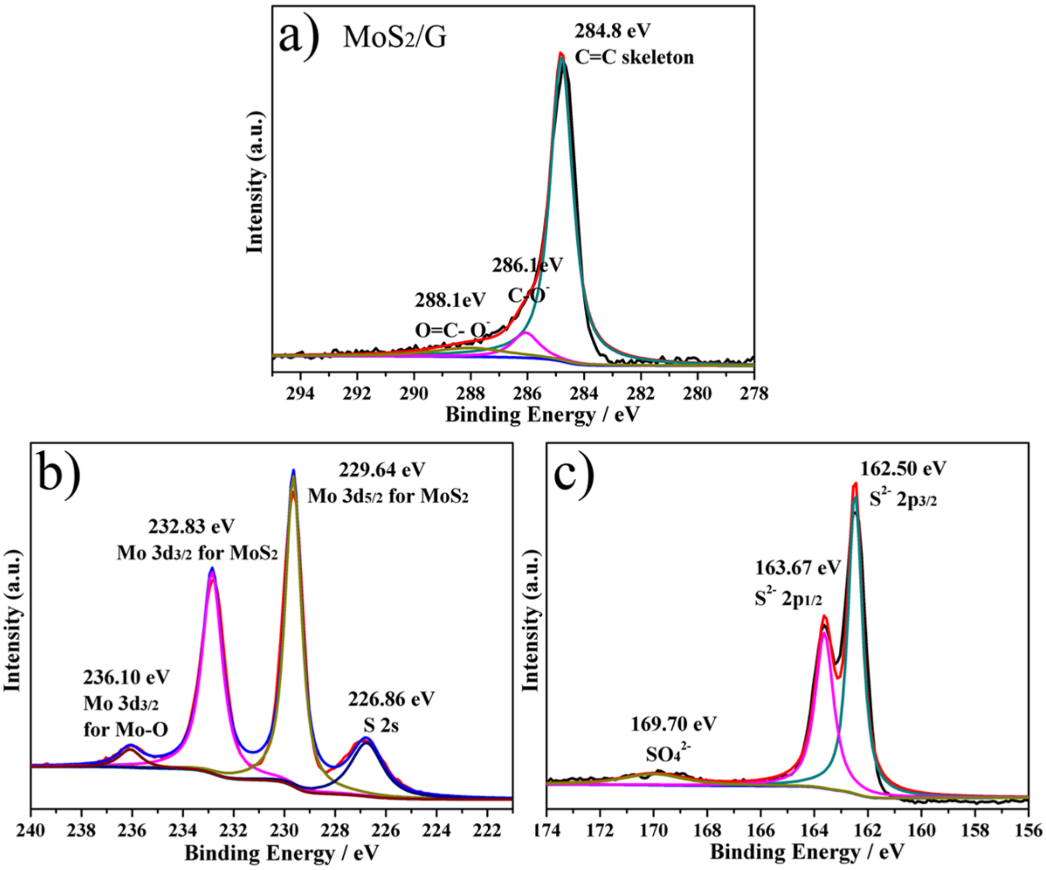

Fig. S20 Core-level XPS spectra of (a) C 1s; (b) Mo 3d and S 2s; (c) S 2p for MoS_2/G.

Table S1. Nitrogen contents and fractions of the N configurations for $MoS_2/NG_{g\text{-}C_3N_4}$ and MoS_2/NG_{urea} in this work, and typical literature reported N-doped graphene.

Samples	***Precursors***	***T***	***N/CN***	***Graphitic N***	***Pyrrolic N***	***Pyridinic N***	***Oxidized N***
$MoS_2/NG_{g\text{-}C_3N_4}$	**GO(50mg)** **$g\text{-}C_3N_4$(100mg)** **$NaMoO_4$(300mg)**	**550°C**	**13 at.%**	**30%**	**15%**	**55%**	--
MoS_2/NG_{urea}	GO(50mg) urea(1 g) $NaMoO_4$(300mg)	550°C	12 at.%	5%	19%	76%	--
NG[4]	GO:melamine (1:5)	800°C *	6.6 at.%	28.59%	8.25%	52.13%	11.03%
NG[5]	GO(50mg) urea(250 mg)	800°C *	7.86 at.%	24%	21.2%	44.4%	10.5%

*It can be seen large fraction of graphitic N formation generally need high temperature above 800°C with less N content (< 10 at.%).

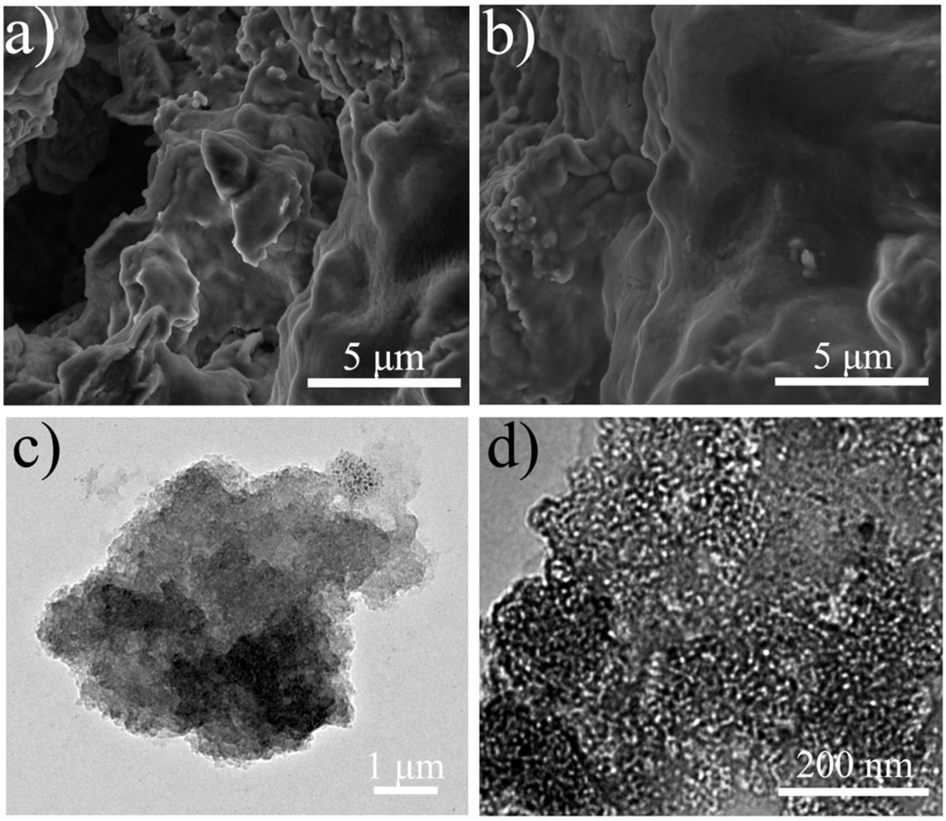

Fig. S21 a,b) SEM images of $MoS_2/NG_{g\text{-}C_3N_4}$ electrode on copper foil after 200 charge and discharge cycles. c,d) TEM images of $MoS_2/NG_{g\text{-}C_3N_4}$ after 200 charge/discharge cycles with well dispersed Mo species.[6]

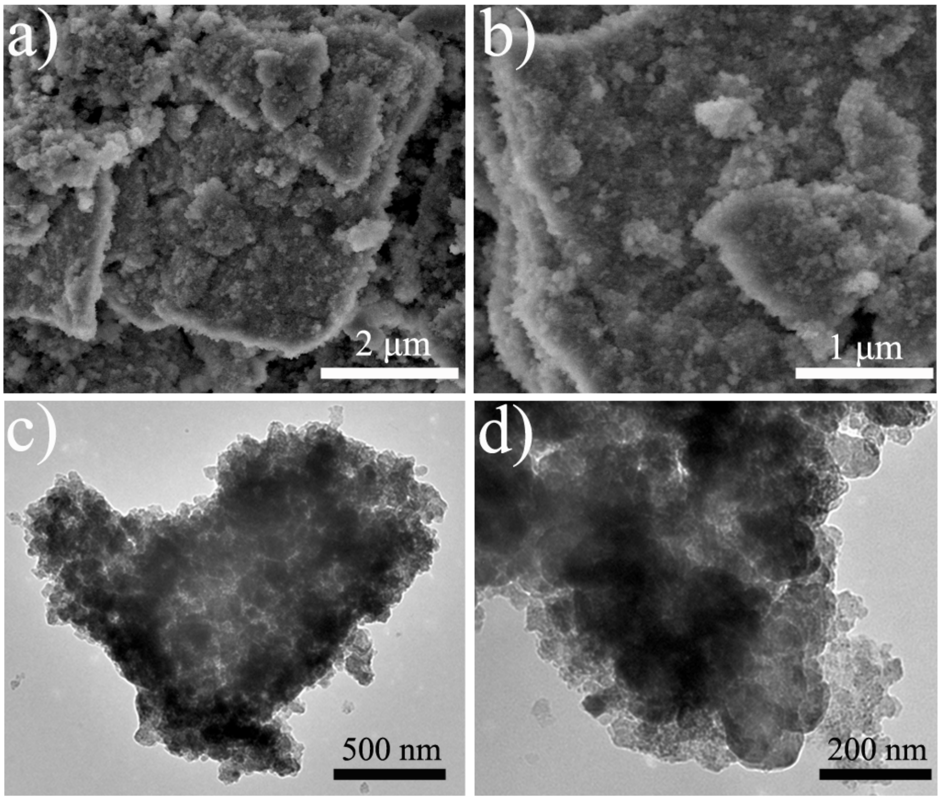

Fig. S22 a,b) SEM images of MoS_2/G electrode on copper foil after 200 charge and discharge cycles. c,d) TEM images of MoS_2/G after 200 charge/discharge cycles .

Table S2. MoS_2 based hybrids (with C or graphene) prepared in this work and the reported literatures and their cycling and rate performances as anode in LIBs

Samples	*Methods*	*Cycling*	*Discharge capacities (mAh g^{-1})*		
			0.1 A/g	*1A/g*	*10 A/g*
$MoS_2/NG_{g\text{-}C_3N_4}$ in this work	**$MoS_3/g\text{-}C_3N_4\text{-}H^+/GO$ treated at 550 °C**	**1450 mAh g^{-1} at 0.1 A/g for 200 cycles**	**1310**	**1200**	**830**
MoS_2/NG_{urea}	MoS_3/GO and urea treated at 550 °C	800 mAh g^{-1} at 0.1 A/g for 200 cycles	840	620	330
MoS_2/G	MoS_3/GO treated at 550 °C	405 mAh g^{-1} at 0.1 A/g after 200 cycles	820	500	160
MoS_2/N-G[1]	N-G prepared at 1050 °C , $NaMoO_4$ and L-cysteine, hydrothermal at	1285 mAh g^{-1} at 0.1 A/g after 50 cycles	1200	850	--

	180°C, finally 800 °C in Ar				
PEO/MoS_2 /Graphene[6]	Exfoliation and restacking	1000 mAh g^{-1} at 0.05 A/g after 180 cycles	900	500	300
3D MoS_2 - graphene[7]	Exfoliation of MoS_2 and hydrothermal with GO at 180°C	1220 mAh g^{-1} at 74 mAh g^{-1} for 30 cycles; 711 mAh g^{-1} at 1860 mA g^{-1}	--	--	--
MoS_2/CCG[8]	Exfoliation and restacking	750 mAh g^{-1} at 0.1 A/g after 50 cycles	957	470	--
MoS_2/3DGN[9]	CVD	877 mAh g^{-1} at 0.1 A/g after 50 cycles	849	597	--
MoS_2/G[10]	hydrothermal at 240 °C, finally 800 °C in Ar	1187 mAh g^{-1} at 0.1 A/g after 100 cycles	1187	900	--
MoS_2/GNS[11]	hydrothermal at 240°C	1290 mAh g^{-1} at 0.1 A/g after 50 cycles	1290	1040	--
GL-MoS_2 / G-CT01[12]	hydrothermal at 240°C, finally 800 °C in N_2	1020 mAh g^{-1} at 0.1 A/g after 100 cycles	1020	760	--
G/MoS_2[13]	hydrothermal at 200°C	1023.7–1234.8 mAh g^{-1} at 0.1 A/g during 100 cycles	1200	848	--
MoS_2 NS/graphene[14]	hydrothermal at 240°C	875 mAh g^{-1} at 832 mAg^{-1} for 50 cycles; 709 mAh g^{-}	--	--	--

		^{1} at 8320 mAg^{-1}			
SL-MoS$_2$-GNS05[15]	refluxed at 95 °C, 800 °C in N$_2$	808 mAh g^{-1} at 0.1 A/g after 100 cycles	900	571	--
CNT@MoS$_2$ NSs[16]	hydrothermal at 200°C, finally 800 °C in H$_2$/N$_2$	698 mAh g^{-1} at 0.1 A/g after 60 cycles	957	369	--
MoS$_2$@CMK-3[17]	hydrothermal at 200°C, 500 °C in H$_2$/N$_2$	934 mAh g^{-1} at 0.4A/g after 150 cycles	893	713	<391
MoS$_2$-carbon fiber[18]	Electrospinning, 450 °C in H$_2$/Ar (5 : 95 v/v), 800 °C under Ar	1000*67% mAh g^{-1} at 1 A/g after 100 cycles	986*67%	637*67%	--
MoS$_2$-C nanotubes[19]	400 °C under H$_2$S	776 mAh g^{-1} at 0.2 A/g after 100 cycles	1100	600	--
N-doped G-SnO$_2$[20]	800 °C under Ar	910 mAh g^{-1} at 50 mA/g after 50 cycles	900	683	--
SnO$_2$ NC@N-RGO[21]	hydrothermal at 200°C and 120°C	1346 mAh g^{-1} at 0.5 A/g after 500 cycles	--	994	631
N-G/Fe$_3$O$_4$[22]	hydrothermal at 180°C , 500 °C under Ar	1130 mAh g^{-1} at 0.1 A/g after 200 cycles	1051	--	<648

(1) Chang, K.; Geng, D.; Li, X.; Yang, J.; Tang, Y.; Cai, M.; Li, R.; Sun, X. Ultrathin MoS$_2$/Nitrogen-Doped Graphene Nanosheets with Highly Reversible Lithium Storage. *Adv. Energy Mater.* **2013**, *3*, 839.

(2) Sun, J.; Zhang, J.; Zhang, M.; Antonietti, M.; Fu, X.; Wang, X. Bioinspired hollow semiconductor nanospheres as photosynthetic nanoparticles. *Nat. Commun.* **2012**, 1139.

(3) Zhuang, X.; Zhang, F.; Wu, D.; Feng, X. Graphene Coupled Schiff-base Porous Polymers: Towards Nitrogen-enriched Porous Carbon Nanosheets with Ultrahigh

Electrochemical Capacity. *Adv. Mater.* **2014**, *26*, 3081.

(4) Sheng, Z.-H.; Shao, L.; Chen, J.-J.; Bao, W.-J.; Wang, F.-B.; Xia, X.-H. Catalyst-Free Synthesis of Nitrogen-Doped Graphene via Thermal Annealing Graphite Oxide with Melamine and Its Excellent Electrocatalysis. *ACS Nano* **2011**, *5*, 4350.

(5) Lin, Z.; Waller, G.; Liu, Y.; Liu, M.; Wong, C.-P. Facile Synthesis of Nitrogen-Doped Graphene via Pyrolysis of Graphene Oxide and Urea, and its Electrocatalytic Activity toward the Oxygen-Reduction Reaction. *Adv. Energy Mater.* **2012**, *2*, 884.

(6) Xiao, J.; Wang, X.; Yang, X.-Q.; Xun, S.; Liu, G.; Koech, P. K.; Liu, J.; Lemmon, J. P. Electrochemically Induced High Capacity Displacement Reaction of PEO/MoS_2/Graphene Nanocomposites with Lithium. *Adv. Funct. Mater.* **2011**, *21*, 2840.

(7) Gong, Y.; Yang, S.; Zhan, L.; Ma, L.; Vajtai, R.; Ajayan, P. M. A Bottom-Up Approach to Build 3D Architectures from Nanosheets for Superior Lithium Storage. *Adv. Funct. Mater.* **2014**, *24*, 125.

(8) Pham, V. H.; Kim, K.-H.; Jung, D.-W.; Singh, K.; Oh, E.-S.; Chung, J. S. Liquid phase co-exfoliated MoS_2-graphene composites as anode materials for lithium ion batteries. *J. Power Sources* **2013**, 244, 280-286.

(9) Cao, X.; Shi, Y.; Shi, W.; Rui, X.; Yan, Q.; Kong, J.; Zhang, H. Preparation of MoS_2-Coated Three-Dimensional Graphene Networks for High-Performance Anode Material in Lithium-Ion Batteries. *Small* **2013**, *9*, 3433.

(10) Chang, K.; Chen, W. l-Cysteine-Assisted Synthesis of Layered MoS_2/Graphene Composites with Excellent Electrochemical Performances for Lithium Ion Batteries. *ACS Nano* **2011**, *5*, 4720.

(11) Chang, K.; Chen, W. In situ synthesis of MoS_2/graphene nanosheet composites with extraordinarily high electrochemical performance for lithium ion batteries. *Chem. Commun.* **2011**, *47*, 4252.

(12) Huang, G.; Chen, T.; Chen, W.; Wang, Z.; Chang, K.; Ma, L.; Huang, F.; Chen, D.; Lee, J. Y. Graphene-Like MoS_2/Graphene Composites: Cationic Surfactant-Assisted Hydrothermal Synthesis and Electrochemical Reversible Storage of Lithium. *Small* **2013**, *9*, 3693.

(13) Yu, H.; Ma, C.; Ge, B.; Chen, Y.; Xu, Z.; Zhu, C.; Li, C.; Ouyang, Q.; Gao, P.; Li, J.; Sun, C.; Qi, L.; Wang, Y.; Li, F. Three-Dimensional Hierarchical Architectures Constructed by Graphene/MoS_2 Nanoflake Arrays and Their Rapid Charging/Discharging Properties as Lithium-Ion Battery Anodes. *Chem. Eur. J.* **2013**, *19*, 5818.

(14) Zhang, K.; Kim, H.-J.; Shi, X.; Lee, J.-T.; Choi, J.-M.; Song, M.-S.; Park, J. H. Graphene/Acid Coassisted Synthesis of Ultrathin MoS_2 Nanosheets with Outstanding Rate Capability for a Lithium Battery Anode. *Inorg. Chem.* **2013**, *52*, 9807.

(15) Wang, Z.; Chen, T.; Chen, W.; Chang, K.; Ma, L.; Huang, G.; Chen, D.; Lee, J. Y.

CTAB-assisted synthesis of single-layer MoS_2-graphene composites as anode materials of Li-ion batteries. *J. Mater. Chem.* A **2013**, *1*, 2202.

(16) Ding, S.; Chen, J. S.; Lou, X. W. Glucose-Assisted Growth of MoS_2 Nanosheets on CNT Backbone for Improved Lithium Storage Properties. *Chem. Eur. J.* **2011**, *17*, 13142.

(17) Xu, X.; Fan, Z.; Yu X.; Ding S,; Yu D.; Lou X. W. A Nanosheets-on-Channel Architecture Constructed from MoS_2 and CMK-3 for High-Capacity and Long-Cycle-Life Lithium Storage. *Adv. Energy Mater.* DOI: 10.1002/aenm.201400902.

(18) Zhu, C.; Mu, X.; van Aken, P. A.; Yu, Y.; Maier, J. Single-Layered Ultrasmall Nanoplates of MoS_2 Embedded in Carbon Nanofibers with Excellent Electrochemical Performance for Lithium and Sodium Storage. *Angew. Chem. Int. Ed.* **2014**, *53*, 2152.

(19) Zhang, C.; Wang, Z.; Guo, Z.; Lou, X. W. Synthesis of MoS_2-C one-dimensional nanostructures with improved lithium storage properties. *ACS Appl. Mater. Interfaces* **2012**, 4, 3765

(20) Wang, X.; Cao, X.; Bourgeois, L.; Guan, H.; Chen, S.; Zhong, Y.; Tang, D. M.; Li, H.; Zhai, T.; Li, L. N-Doped Graphene-SnO_2 Sandwich Paper for High-Performance Lithium-Ion Batteries. *Adv. Funct. Mater.* **2012**, *22*, 2682.

(21) Zhou, X.; Wan, L. J.; Guo, Y. G. Binding SnO_2 Nanocrystals in Nitrogen-Doped Graphene Sheets as Anode Materials for Lithium-Ion Batteries. *Adv. Mater.* **2013**, *25*, 2152.

(22) Chang, Y.; Li, J.; Wang, B.; Luo, H.; He, H.; Song, Q.; Zhi, L. Synthesis of 3D nitrogen-doped graphene/Fe_3O_4 by a metal ion induced self-assembly process for high-performance Li-ion batteries. *J. Mater. Chem. A,* **2013**, 1, 14658.